bioRxiv preprint doi: https://doi.org/10.1101/462259; this version posted November 5, 2018. The copyright holder for this preprint (which was not certified by peer review) is the author/funder, who has granted bioRxiv a license to display the preprint in perpetuity. It is made available under aCC-BY-NC-ND 4.0 International license.

tartan underlies the evolution of male genital morphology

Joanna F. D. Hagen[1], Claudia C. Mendes[1,2], Kentaro M. Tanaka[1,3], Pedro Gaspar[1], Maike Kittelmann[1], Alistair P. McGregor[1,*] and Maria Daniela S. Nunes[1,*]

[1] Department of Biological and Medical Sciences, Oxford Brookes University, Oxford OX3 0BP, United Kingdom.

[2] Present address: Department of Physiology, Anatomy and Genetics, University of Oxford, Oxford OX1 3QX, United Kingdom.

[3] Present address: Department of Biological Sciences, Tokyo Metropolitan University, 1-1 Minami-osawa, Hachioji, 192-0397, Japan.

*Corresponding authors

bioRxiv preprint doi: https://doi.org/10.1101/462259; this version posted November 5, 2018. The copyright holder for this preprint (which was not certified by peer review) is the author/funder, who has granted bioRxiv a license to display the preprint in perpetuity. It is made available under aCC-BY-NC-ND 4.0 International license.

Abstract

Male genital structures are among the most rapidly evolving morphological traits and are often the only features that can distinguish closely related species. This process is thought to be driven by sexual selection and may reinforce the separation of species. However, little is known about the genetic basis for diversification of male genital organs. Indeed, while the causative genetic changes for differences in many phenotypes have been identified, we still lack knowledge about the genes underlying evolutionary differences in traits such as organ size. The claspers (surstyli) are male genital structures that play an important role in copulation in insects. Here we show that natural variation in clasper size and bristle number between *Drosophila mauritiana* and *D. simulans* is caused by evolutionary changes in *tartan* (*trn*), a gene encoding a transmembrane leucine-rich repeat domain protein that mediates cell-cell interactions and affinity differences. There are no fixed amino acid differences in *trn* between *D. mauritiana* and *D. simulans* but differences in the expression of this gene in developing genitalia indicate that these species have evolved cis-regulatory changes in *trn*. Finally, analysis of reciprocal hemizyotes that are genetically identical, except for which species the functional allele of *trn* is from, determined that the *trn* allele of *D. mauritiana* specifies larger claspers than the allele of *D. simulans*. Therefore we have unequivocally identified the first gene underlying the rapid evolution of a male genital organ and a contributor to natural variation in organ size. Moreover, given that *trn* functions as a cell affinity molecule, this may represent a novel mechanism for the evolution of organ size.

bioRxiv preprint doi: https://doi.org/10.1101/462259; this version posted November 5, 2018. The copyright holder for this preprint (which was not certified by peer review) is the author/funder, who has granted bioRxiv a license to display the preprint in perpetuity. It is made available under aCC-BY-NC-ND 4.0 International license.

Introduction

The morphology of male genitalia can differ dramatically even between very closely related animal species (1). In *Drosophila mauritiana* males, for example, the size, shape and bristle morphology of the claspers (surstyli), epandrial lobes (particularly the posterior lobe) and anal plates (cerci) are strikingly different from those of its sister species *D. simulans* and *D. sechellia* (Fig. 1). Moreover, these differences have evolved in only the last 240,000 years since these species last shared a common ancestor (2) (Fig. 1a).

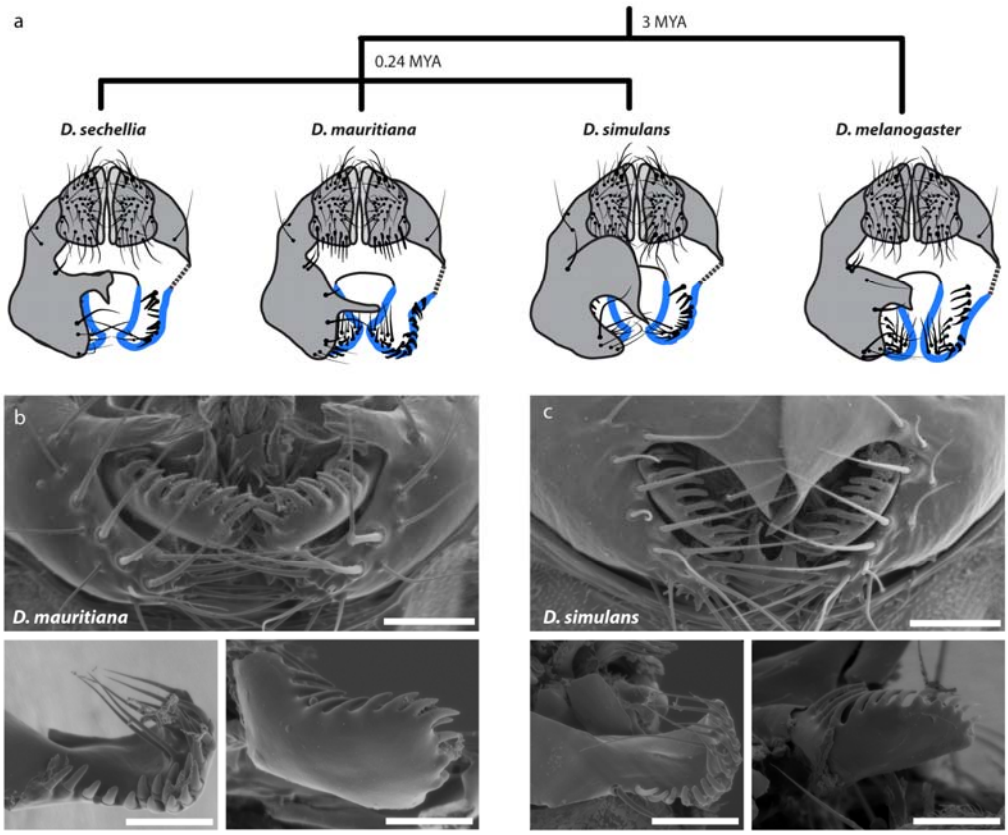

Fig. 1. Divergence in external male terminalia in the *D. simulans* clade and its relationship to the outgroup *D. melanogaster* (2). **a**. Schematic representation of the male analia and genitalia (posterior view). Posterior lobes are illustrated as dissected away on the right-hand-side, in order to facilitate visualisation of the claspers (outlined in blue), which are typically covered by the posterior lobes. While the shape and size of the posterior lobes is species-specific, the claspers and anal plates are very similar between *D. simulans and D. sechellia*, which are smaller and have less bristles than those of *D. mauritiana* and *D. melanogaster*. In addition, the clasper bristles of *D. mauritiana* are shorter and thicker than those of the other three species (3-5). **b and c**. Scanning electron micrographs of *D. mauritiana* (**b**) and *D. simulans* (**c**) external male genitalia (upper panel) and dissected claspers (lower panels) scale bars = 50 um.

The claspers are secondary genital structures with an essential role in grasping and proprioception of the female, and in securing genital coupling (6-12). As in other animal groups (1, 13-15), morphological variation of genital structures is thought to have been

bioRxiv preprint doi: https://doi.org/10.1101/462259; this version posted November 5, 2018. The copyright holder for this preprint (which was not certified by peer review) is the author/funder, who has granted bioRxiv a license to display the preprint in perpetuity. It is made available under aCC-BY-NC-ND 4.0 International license.

driven by sexual selection (16). The mechanism(s) by which male genital morphology might be under sexual selection (female choice, sperm competition or sexual antagonism (14)), and its contribution to reproductive isolation between populations and species, has been difficult to address and resolve both theoretically (17-19) as well as experimentally (20, 21). Genetic manipulation of the evolved loci would allow us to test directly the effect of male genital divergence on mating behaviour and reproductive fitness and should therefore facilitate the empirical study of these questions (9, 22). However, although quantitative mapping studies of morphological differences in male genitalia between species of the *D. simulans* clade were first carried out more than three decades ago (3, 4, 23-28), the genetic basis of male genital divergence between these species has remained elusive. This is due, at least in part, to the large number of loci found to contribute to variation in size and shape of these structures (3, 26, 27). Indeed, many of the best-understood examples of phenotypic evolution represent traits that have a less polygenic basis (29).

Results and Discussion

Previously, we identified two regions on the left arm of chromosome 3 that contribute to differences in clasper size and bristle number between *D. mauritiana* and *D. simulans* (3). Note that clasper bristle number and size are correlated, and therefore bristle number can be used as an indication of effects on size (3). Here, we have generated new recombinant introgression lines between *D. mauritiana* and *D. simulans* to increase the resolution of one of these regions, C2, from approximately 3.5 Mb (3) to 177 kb (Fig. 2; Supplementary File 6). This interval explains about 16.3% of the difference in clasper size (and 37.9% of clasper bristle number) between the two parental species, and contains eight protein-coding genes with orthologs in *D. melanogaster* (Fig. 2; Supplementary File 1a,b).

RNA-Seq data suggests that only one of these genes, *tartan* (*trn*), is expressed in the terminalia of *D. simulans* and *D. mauritiana* at 30 to 50 hours after puparium formation (hAPF) when the difference in clasper morphology develops between these two species (Supplementary File 2). However, if the evolved gene has a very localised pattern of expression it may be below the detection threshold. Therefore, we knocked-down the expression of all genes in the candidate region (with the exception of *CG34429*, for which there was no available UAS line) to test if these positional candidates are involved in clasper development in *Drosophila* using RNAi in *D. melanogaster* (Supplementary File 3). In addition, we knocked-down *CG11279* and *Capricious* (*caps*) - a gene that also encodes a leucine-rich repeat transmembrane protein closely related to *trn* and that functionally

bioRxiv preprint doi: https://doi.org/10.1101/462259; this version posted November 5, 2018. The copyright holder for this preprint (which was not certified by peer review) is the author/funder, who has granted bioRxiv a license to display the preprint in perpetuity. It is made available under aCC-BY-NC-ND 4.0 International license.

overlaps with *trn* in some contexts (30-36). These two genes flank C2, but their cis-regulatory sequences may still be within this region (Fig. 2a).

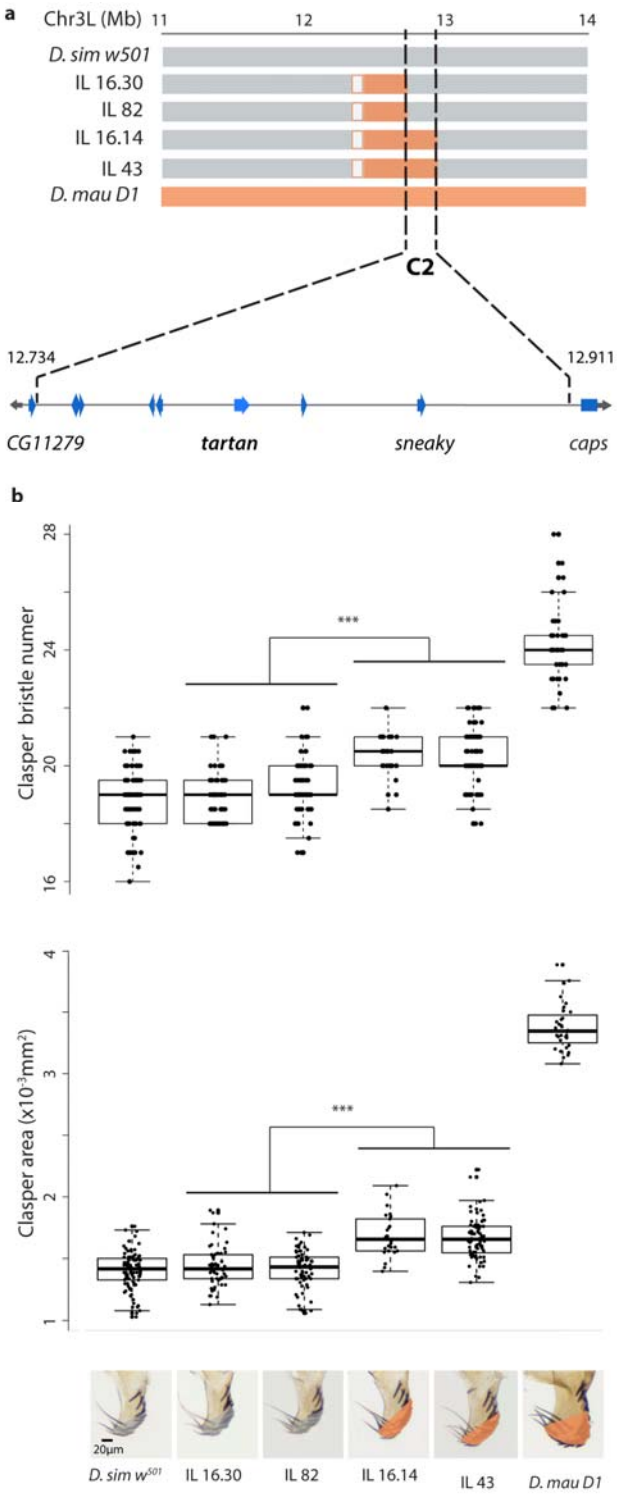

Fig. 2. High-resolution mapping of differences in clasper morphology between *D. simulans* and *D. mauritiana*. a. Introgression line breakpoints on chromosome arm 3L define the 177 kb region C2

bioRxiv preprint doi: https://doi.org/10.1101/462259; this version posted November 5, 2018. The copyright holder for this preprint (which was not certified by peer review) is the author/funder, who has granted bioRxiv a license to display the preprint in perpetuity. It is made available under aCC-BY-NC-ND 4.0 International license.

(grey, orange and white boxes indicate DNA regions from *D. simulans*, *D. mauritiana* or not verified, respectively). Coordinates are given in Mb with respect to the *D. simulans* genome. This region contains eight protein coding genes including *trn* and flanked by *CG11279* and *caps*. **b**. Introgression lines containing region C2 from *D. mauritiana* D1 strain (IL43 and IL16.14) contribute 37.9% of the difference in bristles (upper graph) and 16.3% of the clasper size (lower graph) difference of this species compared to *D. simulans*. Significant differences were detected between IL 43, IL16.14 and IL16.30, IL82 for clasper bristle number (Kruskal-Wallis $p < 0.001$, $X^2_{(5, N = 213.6)}$) and clasper area (ANOVA $p < 0.001$, $F_{(5, 346)} = 823.7$). Asterisks indicate significance comparisons of clasper bristle number (Dunn's test where $p < 0.001$) and clasper area (Tukey's test where $p < 0.001$) (see Supplementary Table 1b). Shading in the bottom panel indicates the area measured at the distal end of the claspers in lines containing *D. simulans* (grey) or *D. mauritiana* regions (orange) for C2. Boxes indicate the range, upper and lower quartiles and median for each sample.

We found that while knockdown of *trn* significantly reduced the size of the claspers (Supplementary File 3 and Extended Data Fig. 1), RNAi against any of the other nine genes, including *caps*, had no effect on clasper morphology in *D. melanogaster* (Supplementary File 3). Note that *trn* RNAi had no effect on the posterior lobes consistent with region C2 only affecting the claspers (Supplementary File 3).

It is thought that the main function of *trn* is to confer differences in affinity between cells and mediate their correct allocation to compartments in developing tissues such as the nervous system, trachea, eyes, wings and legs (30, 31, 35, 37-39). Intriguingly, changes in *trn* expression can affect the allocation of cells between compartments, cause misspecification of compartmental boundaries, and even result in invasive movements of cells across such boundaries (36, 38, 39).

Our RNA-seq data indicates that *trn* is more highly expressed in *D. simulans* than in *D. mauritiana* during terminalia development (Supplementary File 2). To verify this result and investigate the spatial pattern of *trn* throughout development of the terminalia, we performed mRNA *in situ* hybridisation (ISH) in *D. mauritiana* and *D. simulans* (Fig. 3). We observed that *trn* is more highly expressed at the centre of the terminalia, from where the internal genital structures will develop, in *D. simulans* compared to *D. mauritiana* (Fig. 3). However, the expression of *trn* is detected in a wider domain and persists for longer at the base of the developing claspers of *D. mauritiana* compared to *D. simulans* (see black arrowheads in Fig. 3). These results are consistent with both the RNA-Seq data (overall higher expression in the terminalia of *D. simulans*, Supplementary File 2) as well as with the RNAi knockdown results (knockdown of *trn* results in smaller claspers in *D. melanogaster*). Moreover, this suggests that the higher and/or more enduring expression of trn^{mau} allele relative to the trn^{sim} allele in the developing claspers is responsible for the larger claspers in *D. mauritiana* than in *D. simulans*. Furthermore, in situ hybridisation for *CG11279* and *caps*

bioRxiv preprint doi: https://doi.org/10.1101/462259; this version posted November 5, 2018. The copyright holder for this preprint (which was not certified by peer review) is the author/funder, who has granted bioRxiv a license to display the preprint in perpetuity. It is made available under aCC-BY-NC-ND 4.0 International license.

(which are both also expressed in the terminalia, Supplementary File 2) and *CG34429* (which we were unable to knockdown in *D. melanogaster*) showed that only *trn* is expressed in the developing genitalia in a pattern consistent with a role in clasper development and evolution (Extended Data Fig. 2).

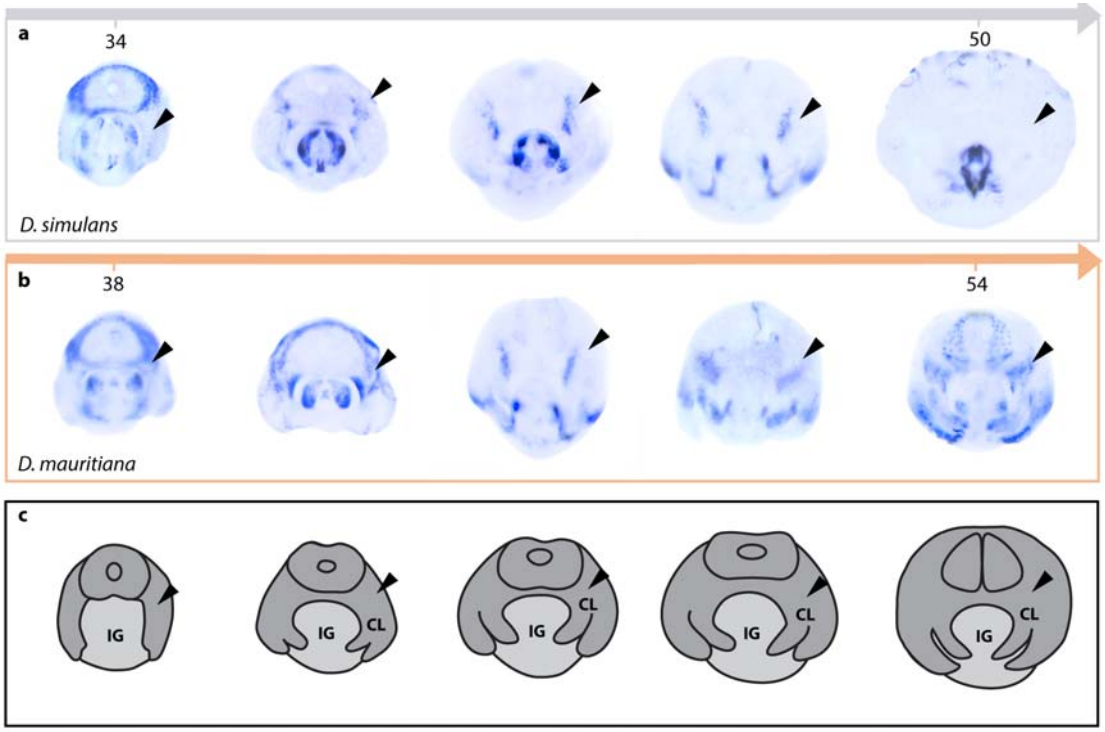

Fig. 3. The spatial and temporal expression of *trn* differs in the developing claspers of *D. simulans* and *D. mauritiana*. Expression shown at four hour intervals hours after puparium formation (hAPF) in *D. simulans* (**a**) and *D. mauritiana* (**b**). **c**. Illustration of the developing structures at each developmental stage. Black arrowheads indicate expression at the base of the developing claspers. Note that genitalia development is approximately 4 hours faster in *D. simulans* than in *D. mauritiana*. IG: Internal Genitalia; CL: Clasper.

There are a total of 22 nucleotide differences in the coding sequence of *trn* between our mapped strains of *D. mauritiana* D1 and *D. simulans* w^{501}, and only three of these are non-synonymous (Supplementary File 4). However, we found that these three amino acid changes are segregating in either or both species. Since we found no fixed amino acid changes between *D. mauritiana* and *D. simulans*, and given the pleiotropic roles of this gene and the difference in expression we observed during clasper development, it is likely that cis-regulatory changes in *trn* underlies the evolution of clasper size between these two species.

Taken together, our mapping, RNAi in *D. melanogaster*, and expression analysis in the developing claspers of *D. mauritiana* and *D. simulans* suggest *trn* underlies differences in clasper morphology. In order to fully test this, we used CRISPR/Cas9 to make null alleles of

bioRxiv preprint doi: https://doi.org/10.1101/462259; this version posted November 5, 2018. The copyright holder for this preprint (which was not certified by peer review) is the author/funder, who has granted bioRxiv a license to display the preprint in perpetuity. It is made available under aCC-BY-NC-ND 4.0 International license.

D. simulans trn w^{501} and *D. mauriana trn* (in IL43, see Fig. 2; Extended Data Fig. 3). We then generated reciprocal hemizyotes for *trn* i.e. genetically identical male flies that differ only in whether they have a functional copy of *trn* from *D. mauritiana* or *D. simulans* (Fig. 4a) (40). Comparison of the claspers between male reciprocal hemizyotes of *trn* shows that flies with a functional *D. mauritiana trn* allele have significantly more clasper bristles and on average 7% larger claspers than those with a functional *D. simulans trn* allele (Fig. 4a). This confirms that, consistent with the effects of the introgressions containing *trn* (Fig. 2), the *D. mauritiana trn* has evolved to confer larger claspers than *D. simulans trn*.

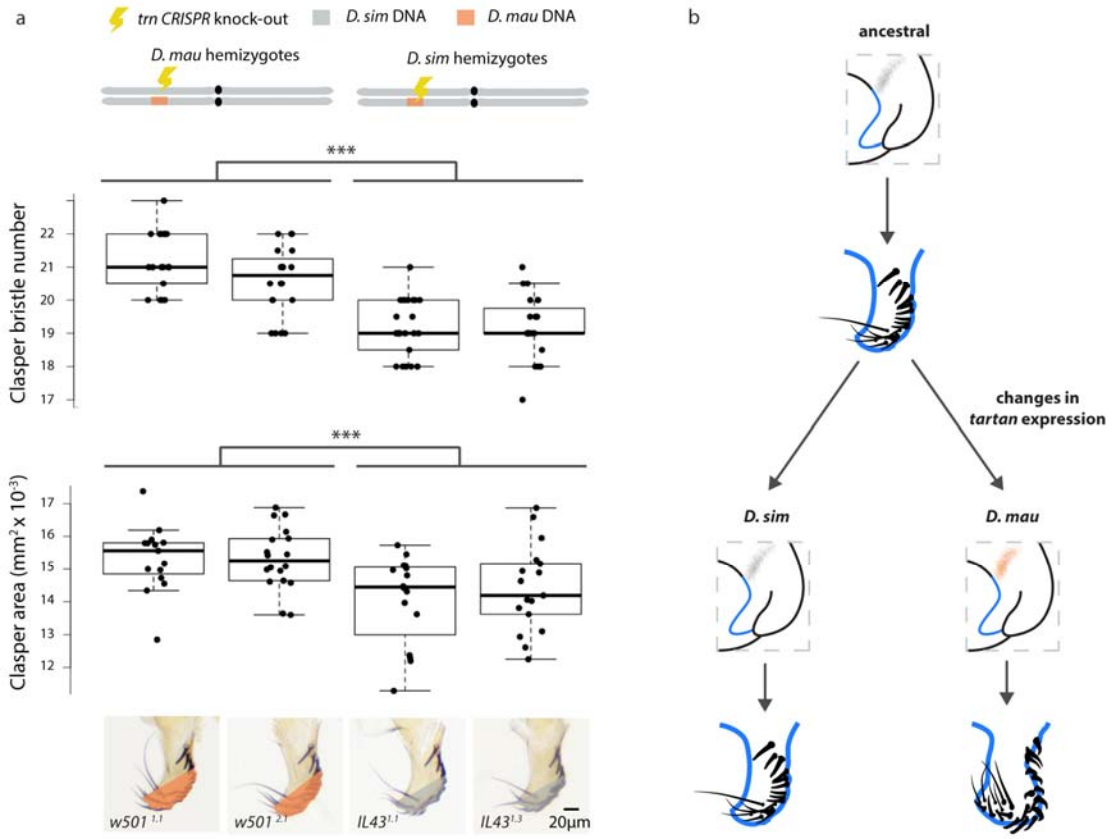

Fig. 4 Reciprocal hemizygotes of *trn* show that this locus contributes to evolutionary differences in male clasper morphology. a. Schematic at the top illustrates the 3rd chromosome of the reciprocal hemizygotes carrying a functional allele of *trn* from only *D. mauritiana* (left) or *D. simulans* (right). The graphs shows clasper bristle number size of two *D. mauritiana trn* hemizygote lines compared to two *D. simulans* hemizygote lines (with images of representative claspers from each line with the area measured in grey (*D. simulans* hemizygotes) or orange (*D. mauritiana* hemizygote)). The *D. mauritiana trn* allele confers claspers with more bristles (one tailed *t*-test $p < 0.001$, t (85) = 8.51 and a larger area (one tailed *t*-test $p < 0.001$, t (57) = 3.29) compared to the *D. simulans trn* allele. Asterisks indicate t – test comparisons with significance value of $p < 0.001$. Boxes show the range, upper and lower quartiles, and the median for each sample. b. Evolutionary changes in the spatial and/or temporal expression of *trn* during clasper development in *D. mauritiana* have led to larger claspers with more bristles in this species compared to *D. simulans.*

bioRxiv preprint doi: https://doi.org/10.1101/462259; this version posted November 5, 2018. The copyright holder for this preprint (which was not certified by peer review) is the author/funder, who has granted bioRxiv a license to display the preprint in perpetuity. It is made available under aCC-BY-NC-ND 4.0 International license.

trn is the first gene to be identified that underlies the rapid evolution in the size of a male genital organ and more generally one of the first loci found to contribute to natural variation in organ size. While there are many examples of phenotypic evolution caused by changes in the expression of transcription factors and signalling molecules (29), including differences in genital bristles between other *Drosophila* species (41), *trn* encodes a leucine-rich repeat domain transmembrane (30, 31, 35, 36, 38, 42). *trn* appears to mediate affinity differences in cell-cell contact directly through its extracellular domain, directing mispositioned cells towards unknown cues (36, 38). Our results suggest that differences in *trn* expression in *Drosophila* are able to alter clasper size. Therefore, changes in cell affinity caused by variation in the temporal and/or spatial expression of transmembrane proteins that mediate cell affinity may represent a new mechanism for the evolution of organ size. However, there is also some evidence that *trn* could act as a ligand and may transduce signals, although its intracellular domain appears to be dispensable for most of its functions (30, 35, 36, 42). Therefore, further study into the function of *trn* and characterisation of its role in organ size regulation and evolution is required.

Methods

Introgression mapping and phenotyping

We generated new recombinants from introgression line D11.01, which contains *D. mauritiana* w^- DNA in the genomic location 3L:7527144...15084689 Mb, encompassing the candidate regions C1 and C2 (3). To increase the resolution of the candidate region C2 (3) we backcrossed virgin D11.01/*D. simulans* w^{501} heterozygous females to *D. simulans* w^{501} males and selected against the visible marker D1 (3, 43) but retained *D. mauritiana* DNA in the predicted C2 region by genotyping with molecular markers (Supplementary Files 5 and 6). Novel recombinants were identified using restriction fragment length polymorphisms (RFLPs) and then maintained as homozygous stocks. Flies were phenotyped and genotyped as described previously (3), using molecular markers (Supplementary File 5). All stocks and crosses were maintained on a standard cornmeal diet at 25°C under a 12-h:12-h dark/light cycle unless otherwise stated.

The posterior lobes were dissected away from the claspers and anal plates, and T1 legs were also retained. The claspers and T1 tibia were mounted in Hoyer's medium, and images were taken using a Zeiss Axioplan light microscope at X250 magnification for the claspers and X125 for the T1 legs, using a DFC300 camera. Clasper area (see shaded area in Fig. 1b) and tibia length were measured manually using ImageJ (44), and bristle number

bioRxiv preprint doi: https://doi.org/10.1101/462259; this version posted November 5, 2018. The copyright holder for this preprint (which was not certified by peer review) is the author/funder, who has granted bioRxiv a license to display the preprint in perpetuity. It is made available under aCC-BY-NC-ND 4.0 International license.

counted for each clasper. T1 tibia length was used as a proxy for body size, in order to control for the consistency in rearing conditions. Most introgression lines showed no difference in T1 tibia length (Supplementary File 1), and since genitalia are hypoallometric (22, 25, 26, 45-47), the phenotypic data was not further corrected for body size.

We first tested the normality of the introgression lines duplicates. Depending on the result of this analysis, we conducted either a Kruskal-Wallis followed by a Dunns test, or an ANOVA followed by a Tukey's test in order to determine any significant differences between duplicates. If duplicates were not significantly different from each other, the phenotypic measurements were merged. We then compared the phenotype of each the introgression lines to the parental *D. simulans* w^{501} line using a Dunnett's test (Supplementary File 1a). Region C2 was determined by conducting a Kruskal-Wallis followed by a Dunn's test (clasper bristle number) and an ANOVA followed by Tukey's test (clasper area) between IL 43, IL16.14 and IL30, IL82 (Supplementary File 1b). The effect of introgression lines was calculated as a percentage of the difference between the parental *D. simulans* and *D. mauritiana* strains and was averaged over all lines used to map C2 to determine final effect size (Supplementary File 1a). All statistical analyses were conducted in R Studio.

Scanning electron microscopy

For intact male *Drosophila* genitalia, the fly heads were removed and flies placed into fixative (2% PFA, 2.5% GA in 0.1M NaCac buffer) for 2 hours. To visualise the claspers genitalia were dissected in Hoyer's and then placed into fixative. Samples were washed in water and fixed in 1% Osmium over night at 4°C. Osmium was removed, flies washed with water and then taken through a series of ethanol dilutions up to 100% ethanol for dehydration. After 24 hours of 100% ethanol, flies were processed in a critical point dryer and mounted to SEM stubs with Conductive Silver Epoxy (Chemtronics) or coated carbon tabs and gold coated for 30 sec using a sputter coater. Genitalia were imaged at 2560 × 1920 px in a Hitachi S-3400N SEM in SE mode at 5kV. Working distance ranged between 7 and 10 mm.

RNA sequencing and differential expression analysis

We generated three independent biological replicates of RNA-Seq libraries for *D. simulans* w^{501} and *D. mauritiana w* terminalia. Males were collected at the white pupal stage by sorting gonad size and placed in a humid chamber, and dissected at 30 and 50 hAPF. Because early pupal tissues are soft, we flash froze the whole pupae by placing on cooled aluminium block

bioRxiv preprint doi: https://doi.org/10.1101/462259; this version posted November 5, 2018. The copyright holder for this preprint (which was not certified by peer review) is the author/funder, who has granted bioRxiv a license to display the preprint in perpetuity. It is made available under aCC-BY-NC-ND 4.0 International license.

with a cake of dry ice. Abdominal tips from 20–30 males were collected to extract the total RNA per biological replicate. The total RNA was extracted using TRIzol Plus RNA Purification Kit (Life Technologies). The samples were DNaseI (Invitrogen) treated to avoid DNA contamination and the RNA quality was checked using TapeStation (Agilent Technologies). Using 300 ng of total RNA, indexed libraries were generated using the combination of KAPA Stranded mRNA-Seq Kit (KAPA Biosystems) and Adapter Kit (FastGene). Indexed libraries were sent to the Macrogen Japan for sequencing in single lane of HiSeq4000 (Illumina), producing 100 bp paired-end reads. Raw fastq files were quality controlled by FastQCs (ver. 1.34) with the following criterion: minimum length 50 bp, the average Q-score > 20, and continuous base "N" < 2. Filtered reads were mapped to reference coding sequence (CDS) set from(48) using Bowtie2 (ver. 2.2.9). Read counts per CDS were extracted using Samtools (ver. 1.3.1) and the reads per kilo base per million mapped reads (RPKM) were calculated. Raw fastq files are deposited at DDBJ under the accession numbers DRA006755 and DRA006758 for *D. mauritiana* and *D. simulans*, respectively. Genes were considered not to be expressed if RKPM was below 1.5.

RNAi knockdown of C2 candidate genes

We conducted an RNAi knock down of all the genes within region C2 (with the exception *CG34429* for which there was no available UAS line) in *D. melanogaster* using UAS-RNAi lines from both Vienna Drosophila RNAi Center and TRiP lines from Bloomington stock center (Supplementary File 7). UAS males of our candidate genes were crossed to female NP6333–GAL4 driver virgins (P(GawB)PenNP6333) (49) carrying the transgene UAS-Dicer-2 P(UAS-Dcr-2.D). Crosses for the RNAi were carried out at 25°C. The genital morphology of the male knockdowns was compared to NP6333-Gal4; UAS-Dicer and UAS-RNAi controls. Clasper bristle number and tibia length were measured for 16 individuals of each genotype. Differences in clasper bristle number and tibia size were assessed using a one-way ANOVA followed by a Tukey's test (Supplementary File 3).

Sequence analysis

To evaluate if any of the nucleotide differences in the coding sequence of *trn* were fixed between species we took advantage of two population datasets available for *D. simulans* and *D. mauritiana*. One of these datasets consists of Pool-seq data from 107 strains of *D. mauritiana* and from 50 strains of sub-Saharan *D. simulans* (50, 51) available at http://www.popoolation.at/pgt/. To compare allele frequency at the same sites between the

bioRxiv preprint doi: https://doi.org/10.1101/462259; this version posted November 5, 2018. The copyright holder for this preprint (which was not certified by peer review) is the author/funder, who has granted bioRxiv a license to display the preprint in perpetuity. It is made available under aCC-BY-NC-ND 4.0 International license.

two Pool-seq datasets we used a script, kindly provided by Ram Pandey, that aligns the genomes of both species using MAUVE (52) and retrieves the corresponding coordinates and allele frequency information. The data for the coding sequence of tartan is shown in Supplementary File 4. The other dataset consists of whole genome data for ten strains of each species submitted to the SRA database by the University of Rochester (*D. mauritiana* lines: SRX135546, SRX688576, SRX688581, SRX688583, SRX688588, SRX688609, SRX688610, SRX688612, SRX688710, SRX688712; *D. simulans* lines: SRX497551, SRX497574, SRX497553, SRX497563, SRX497558, SRX497564, SRX497559, SRX495510, SRX495507, SRX497557). An alignment of the *trn* region was kindly provided by the Presgraves lab and is included in the Supplementary File 8. We resequenced 3.6 kb of the *trn* gene region in *D. simulans* w^{501} and *D. mauritiana* D1 (trn-1 to trn4 primers in Supplementary File 5). The sequence analysis is summarized in Supplementary File 4.

In situ hybridisation

Staged male pupae which had been incubated at 25°C were flash-frozen on a metal heat block cooled to -80°C. The posterior third of the pupae were cut off and fixed in 4% paraformaldehyde/PBT for half an hour, and washed in methanol and stored at -20'C. Before the *in situ*, the vitellin membranes were peeled away in ice cold methanol. Note that the stages collected in *D. simulans* and *D. mauritiana* are different, due to our observation that our D1 *D. mauritiana* strain develops approximately 4 hours more slowly than *D. simulans* w^{501} (data not shown).

Total RNA was extracted from *D. mauritiana* D1, *D. simulans* w^{501} and *D. melanogaster* w^{1118} at a range of developmental time-points using Trizol extraction. A Quantitect Reverse Transcription Kit (Qiagen) was used to synthesize cDNA, in which gene-specific fragments were amplified separately for each species. Primers for *trn*, *CG11279*, *CGCG34429* and *caps* were designed using Primer3 (http://primer3.ut.ee) with the addition of T7 linker sequences added to the 5' end of each primer. To FWD primers (sense) and REV primers (antisense) we added ggccgcgg and cccggggc respectively. Primers are as follows; *trn* (514 bp) ATCGAGGAGCTGAATCTGGG and TCCAGGTTACCATTGTCGCT, *CG11279* (458 bp) CATCTCGAAGTCGGTCAACA and AGGGTCACCTGACCATCAAT, *CGCG34429* (393 bp) GGCTTTGGTATACCTGCAGAA and TGAGCAGGATGTGAAGCACT and *caps* (520 bp) CCGGGAGAACTAACCTTCCA and CTTCATCCAGGCTGCTCAAC. Probes were labeled with 10x DIG labelling mix (Roche

bioRxiv preprint doi: https://doi.org/10.1101/462259; this version posted November 5, 2018. The copyright holder for this preprint (which was not certified by peer review) is the author/funder, who has granted bioRxiv a license to display the preprint in perpetuity. It is made available under aCC-BY-NC-ND 4.0 International license.

Diagnostics) and T7 RNA polymerase (Roche Diagnostics). Purple/dark blue staining was detected using alkaline phosphatase-conjugated anti-DIG antibody FAB fragments (Roche Diagnostics) and Nitro Blue tetrazolium/5-bromo-4-chloro-3-indolyl-phosphate NBT/BCIP (Roche Diagnostics). In situ hybridizations were based on the Carroll lab "Drosophila abdominal in situ" protocol (http://carroll.molbio.wisc.edu/methods.html) with minor modifications.

Generation of reciprocal hemizygotes and statistical analysis

We generated a double-stranded cut 121 bp into the first coding exon of *trn*, resulting in a frameshift mutation. The cut was mediated by pCFD3 gRNA plasmid and pHD-DsRed-attp donor plasmid co-injected by The University of Cambridge Department of Genetics Fly Facility at 0.1ug/ul and 0.5ug/ul respectively, into *D. simulans* w^{501} and IL43 which endogenously express Cas9 from the X chromosome. These strains were generated by introgressing the X chromosome from *y w* p{nos-Cas9, w^{+}} in pBac{3XP3::EYFP,attp} sim 1087, which was kindly provided by David Stern (53). The cut site of two transgenic stocks were verified from each of the injected strains (Extended Data Figure 3a and 3b). Transgenic *D. simulans* w^{501} and IL43 males heterozygous for the mutation were then crossed to non-injected IL43 and *D. simulans* w^{501} virgins respectively. These crosses were amplified and the F1 males carrying the mutation (hemizygous for *trn* allele) were phenotyped as described previously (Extended Data Figure 3c).

In order to assess the effect of *trn* reciprocal hemizygotes to clasper phenotype, we first tested for normality and merged measurements from identical *trn* reciprocal hemizygotes (as described previously). We then conducted one-tailed, unpaired *t*-test for both clasper bristle number (unequal variance) and clasper area (equal variance) between reciprocal hemizygotes. Differences in posterior lobe area and tibia length was assessed using a two-tailed, unpaired *t*-test with unequal variance (Supplementary File 1c).

Data Availability

The RNA-Seq data is available at DDBJ under the accession numbers DRA006755 and DRA006758. All other data is provided in the figures, extended data or in supplementary files.

bioRxiv preprint doi: https://doi.org/10.1101/462259; this version posted November 5, 2018. The copyright holder for this preprint (which was not certified by peer review) is the author/funder, who has granted bioRxiv a license to display the preprint in perpetuity. It is made available under aCC-BY-NC-ND 4.0 International license.

References

1. Eberhard WG (1985) *Sexual selection and animal genitalia* (Harvard University Press, Cambridge, Mass.) pp x, 244 p.
2. Garrigan D, *et al.* (2012) Genome sequencing reveals complex speciation in the Drosophila simulans clade. *Genome Res* 22(8):1499-1511.
3. Tanaka KM, *et al.* (2015) Genetic architecture and functional characterization of genes underlying the rapid diversification of male external genitalia between Drosophila simulans and Drosophila mauritiana. *Genetics* 200(1):357-369.
4. True JR, Liu J, Stam LF, Zeng Z-B, & Laurie CC (1997) Quantitative genetic analysis of divergence in male secondary sexual traits between *Drosophila simulans* and *Drosophila mauritiana*. *Evolution* 51:816-832.
5. Tsacas L & David J (1974) *Drosophila mauritiana* n. sp. du groupe melanogaster de I'lle Maurice. *Bulletin de la Societe entomologique de France* 79:42-46.
6. Acebes A, Cobb M, & Ferveur JF (2003) Species-specific effects of single sensillum ablation on mating position in Drosophila. *J Exp Biol* 206(Pt 17):3095-3100.
7. Jagadeeshan S & Singh RS (2006) A time-sequence functional analysis of mating behaviour and genital coupling in Drosophila: role of cryptic female choice and male sex-drive in the evolution of male genitalia. *J Evol Biol* 19(4):1058-1070.
8. Kamimura Y & Mitsumoto H (2011) Comparative copulation anatomy of the *Drosophila melanogaster* species complex (Diptera: Drosophilidae). *Entomological Science* 14:399-410.
9. Masly JP & Kamimura Y (2014) Asymmetric mismatch in strain-specific genital morphology causes increased harm to Drosophila females. *Evolution* 68(8):2401-2411.
10. Mattei AL, Riccio ML, Avila FW, & Wolfner MF (2015) Integrated 3D view of postmating responses by the Drosophila melanogaster female reproductive tract, obtained by micro-computed tomography scanning. *Proc Natl Acad Sci U S A* 112(27):8475-8480.
11. Robertson HM (1988) Mating Asymmetries and Phylogeny in the *Drosophila melanogaster* Species Complex. *Pacific Science* 42:72-80.
12. Yassin A & Orgogozo V (2013) Coevolution between Male and Female Genitalia in the Drosophila melanogaster Species Subgroup. *PLoS One* 8(2).
13. Hosken DJ & Stockley P (2004) Sexual selection and genital evolution. *Trends Ecol Evol* 19(2):87-93.
14. Simmons LW (2014) Sexual selection and genital evolution. *Austral Entomology* 53(1):1-17.
15. Eberhard WG (2010) Evolution of genitalia: theories, evidence, and new directions. *Genetica* 138(1):5-18.
16. House CM, *et al.* (2013) Sexual and natural selection both influence male genital evolution. *PLoS One* 8(5):e63807.
17. Panhuis TM, Butlin R, Zuk M, & Tregenza T (2001) Sexual selection and speciation. *Trends Ecol Evol* 16(7):364-371.
18. Ritchie MG (2007) Sexual Selection and Speciation. *Annual Review of Ecology, Evolution, and Systematics* 38(1):79-102.
19. Servedio MR & Burger R (2014) The counterintuitive role of sexual selection in species maintenance and speciation. *Proc Natl Acad Sci U S A* 111(22):8113-8118.

bioRxiv preprint doi: https://doi.org/10.1101/462259; this version posted November 5, 2018. The copyright holder for this preprint (which was not certified by peer review) is the author/funder, who has granted bioRxiv a license to display the preprint in perpetuity. It is made available under aCC-BY-NC-ND 4.0 International license.

20. Frazee SR & Masly JP (2015) Multiple sexual selection pressures drive the rapid evolution of complex morphology in a male secondary genital structure. *Ecol Evol* 5(19):4437-4450.
21. LeVasseur-Viens H, Polak M, & Moehring AJ (2015) No evidence for external genital morphology affecting cryptic female choice and reproductive isolation in Drosophila. *Evolution* 69(7):1797-1807.
22. Tanaka KM, Kamimura Y, & Takahashi A (2018) Mechanical incompatibility caused by modifications of multiple male genital structures using genomic introgression in Drosophila. *Evolution*.
23. Laurie CC, True JR, Liu J, & Mercer JM (1997) An introgression analysis of quantitative trait loci that contribute to a morphological difference between Drosophila simulans and D. mauritiana. *Genetics* 145(2):339-348.
24. LeVasseur-Viens H & Moehring AJ (2014) Individual Genetic Contributions to Genital Shape Variation between Drosophila simulans and D. mauritiana. *Int J Evol Biol* 2014:808247.
25. Liu J, *et al.* (1996) Genetic analysis of a morphological shape difference in the male genitalia of Drosophila simulans and D. mauritiana. *Genetics* 142(4):1129-1145.
26. Masly JP, Dalton JE, Srivastava S, Chen L, & Arbeitman MN (2011) The genetic basis of rapidly evolving male genital morphology in Drosophila. *Genetics* 189(1):357-374.
27. Zeng ZB, *et al.* (2000) Genetic architecture of a morphological shape difference between two drosophila species. *Genetics* 154(1):299-310.
28. Coyne JA (1983) Genetic basis of differences in genital morphology among three sibling species of Drosophila. *Evolution* 37:1101-1118.
29. Martin A & Orgogozo V (2013) The Loci of repeated evolution: a catalog of genetic hotspots of phenotypic variation. *Evolution* 67(5):1235-1250.
30. Chang Z, *et al.* (1993) Molecular and genetic characterization of the Drosophila tartan gene. *Dev Biol* 160(2):315-332.
31. Mao Y, Kerr M, & Freeman M (2008) Modulation of Drosophila retinal epithelial integrity by the adhesion proteins capricious and tartan. *PLoS One* 3(3):e1827.
32. Shishido E, Takeichi M, & Nose A (1998) Drosophila synapse formation: regulation by transmembrane protein with Leu-rich repeats, CAPRICIOUS. *Science* 280(5372):2118-2121.
33. Kurusu M, *et al.* (2008) A screen of cell-surface molecules identifies leucine-rich repeat proteins as key mediators of synaptic target selection. *Neuron* 59(6):972-985.
34. Hong W, *et al.* (2009) Leucine-rich repeat transmembrane proteins instruct discrete dendrite targeting in an olfactory map. *Nat Neurosci* 12(12):1542-1550.
35. Krause C, Wolf C, Hemphala J, Samakovlis C, & Schuh R (2006) Distinct functions of the leucine-rich repeat transmembrane proteins capricious and tartan in the Drosophila tracheal morphogenesis. *Dev Biol* 296(1):253-264.
36. Milan M, Perez L, & Cohen SM (2005) Boundary formation in the Drosophila wing: functional dissection of Capricious and Tartan. *Dev Dyn* 233(3):804-810.
37. Milan M, Perez L, & Cohen SM (2002) Short-range cell interactions and cell survival in the Drosophila wing. *Dev Cell* 2(6):797-805.
38. Milan M, Weihe U, Perez L, & Cohen SM (2001) The LRR proteins capricious and Tartan mediate cell interactions during DV boundary formation in the Drosophila wing. *Cell* 106(6):785-794.
39. Sakurai KT, Kojima T, Aigaki T, & Hayashi S (2007) Differential control of cell affinity required for progression and refinement of cell boundary during Drosophila leg segmentation. *Dev Biol* 309(1):126-136.

bioRxiv preprint doi: https://doi.org/10.1101/462259; this version posted November 5, 2018. The copyright holder for this preprint (which was not certified by peer review) is the author/funder, who has granted bioRxiv a license to display the preprint in perpetuity. It is made available under aCC-BY-NC-ND 4.0 International license.

40. Stern DL (2014) Identification of loci that cause phenotypic variation in diverse species with the reciprocal hemizygosity test. *Trends Genet* 30(12):547-554.
41. Nagy O, *et al.* (2018) Correlated Evolution of two Sensory Organs via a Single Cis-Regulatory Nucleotide Change. *bioRxiv*.
42. Bugga L, Ratnaparkhi A, & Zinn K (2009) The Cell Surface Receptor Tartan Is a Potential In Vivo Substrate for the Receptor Tyrosine Phosphatase Ptp52F. *Molecular and Cellular Biology* 29(12):3390-3400.
43. True JR, Mercer JM, & Laurie CC (1996) Differences in crossover frequency and distribution among three sibling species of Drosophila. *Genetics* 142(2):507-523.
44. Schneider CA, Rasband WS, & Eliceiri KW (2012) NIH Image to ImageJ: 25 years of image analysis. *Nature methods* 9(7):671-675.
45. Coyne JA, Rux J, & David JR (1991) Genetics of Morphological Differences and Hybrid Sterility between Drosophila-Sechellia and Its Relatives. *Genet Res* 57(2):113-122.
46. Macdonald SJ & Goldstein DB (1999) A quantitative genetic analysis of male sexual traits distinguishing the sibling species Drosophila simulans and D. sechellia. *Genetics* 153(4):1683-1699.
47. Shingleton AW, Estep CM, Driscoll MV, & Dworkin I (2009) Many ways to be small: different environmental regulators of size generate distinct scaling relationships in Drosophila melanogaster. *Proc Biol Sci* 276(1667):2625-2633.
48. Torres-Oliva M, Almudi I, McGregor AP, & Posnien N (2016) A robust (re-)annotation approach to generate unbiased mapping references for RNA-seq-based analyses of differential expression across closely related species. *BMC Genomics* 17:392.
49. Chatterjee SS, Uppendahl LD, Chowdhury MA, Ip PL, & Siegal ML (2011) The female-specific doublesex isoform regulates pleiotropic transcription factors to pattern genital development in Drosophila. *Development* 138(6):1099-1109.
50. Nolte V, Pandey RV, Kofler R, & Schlotterer C (2013) Genome-wide patterns of natural variation reveal strong selective sweeps and ongoing genomic conflict in Drosophila mauritiana. *Genome Res* 23(1):99-110.
51. Pandey RV, Kofler R, Orozco-terWengel P, Nolte V, & Schlotterer C (2011) PoPoolation DB: a user-friendly web-based database for the retrieval of natural polymorphisms in Drosophila. *BMC genetics* 12:27.
52. Darling AE, Mau B, & Perna NT (2010) progressiveMauve: multiple genome alignment with gene gain, loss and rearrangement. *PLoS One* 5(6):e11147.
53. Stern DL, *et al.* (2017) Genetic and Transgenic Reagents for Drosophila simulans, D. mauritiana, D. yakuba, D. santomea, and D. virilis. *G3 (Bethesda)* 7(4):1339-1347.

bioRxiv preprint doi: https://doi.org/10.1101/462259; this version posted November 5, 2018. The copyright holder for this preprint (which was not certified by peer review) is the author/funder, who has granted bioRxiv a license to display the preprint in perpetuity. It is made available under aCC-BY-NC-ND 4.0 International license.

Acknowledgements

We thank Christian Schlötterer, Christina Muirhead and Daven Presgraves for facilitating access to population genetic data, and Amber Blogg and Alex Payne for technical assistance. This work was funded by grants from the NERC (NE/M001040/1) and BBSRC (BB/M020967/1) to APM and a JSPS KAKENHI (15J05233) grant to KMT.

Author contributions

M.D.S.N., A.P.M., J.F.D.H. and P.G. designed the experiments. M.D.S.N., A.P.M. supervised and K.M.T., M.D.S.N., A.P.M. contributed reagents to the project. J.F.D.H., M.D.S.N. and C.C.M. performed the introgression mapping and RNAi experiments. J.F.D.H. and M.K carried out morphological analyses and SEM. K.M.T. performed the RNA-Seq experiments and analysis. J.F.D.H. performed all other experiments. J.F.D.H. and M.D.S.N. analysed the data. M.D.S.N., A.P.M and J.F.D.H wrote the manuscript. All authors read and commented on the manuscript.

bioRxiv preprint doi: https://doi.org/10.1101/462259; this version posted November 5, 2018. The copyright holder for this preprint (which was not certified by peer review) is the author/funder, who has granted bioRxiv a license to display the preprint in perpetuity. It is made available under aCC-BY-NC-ND 4.0 International license.

Supplementary Figures

Supplementary Figure 1.

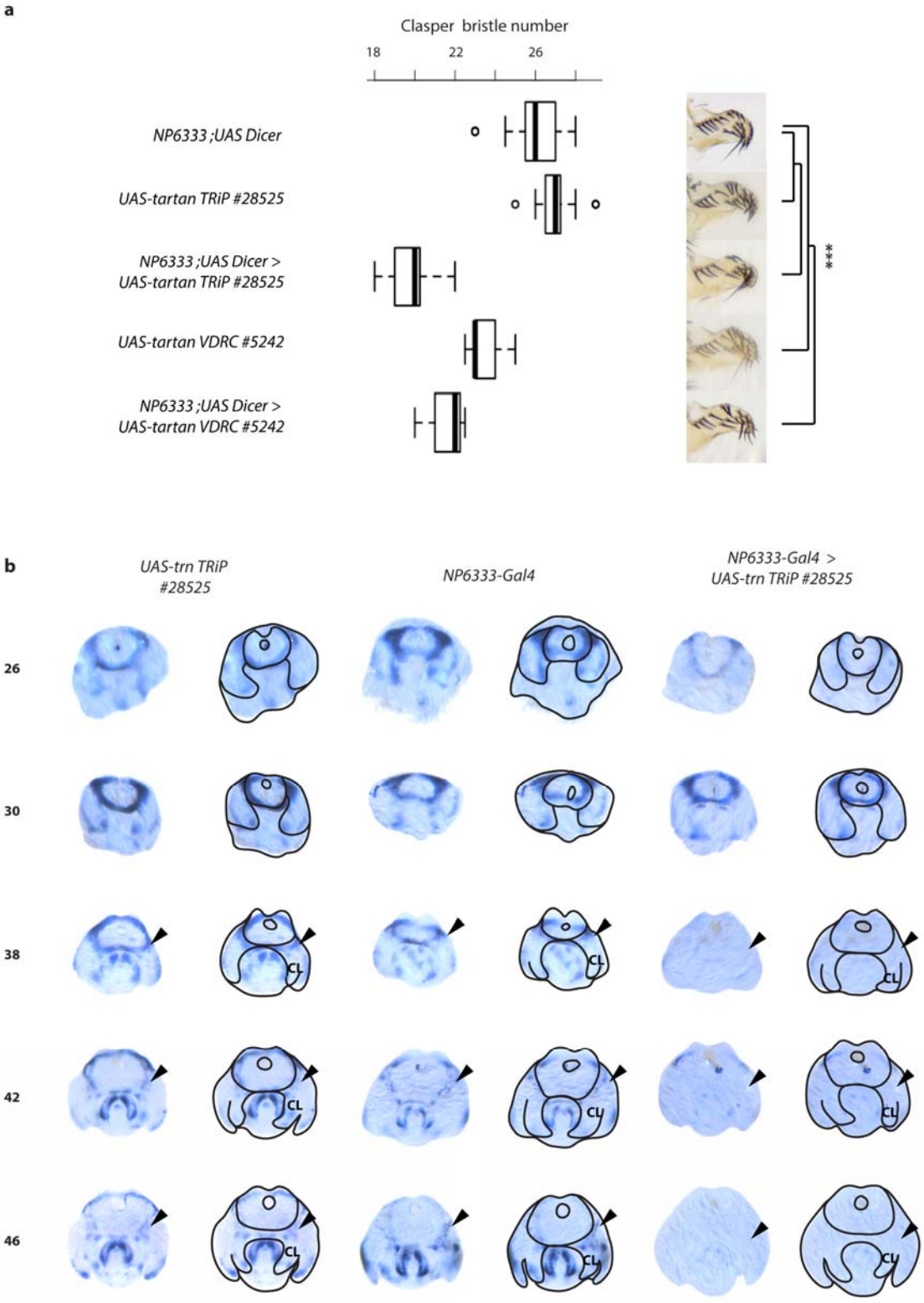

bioRxiv preprint doi: https://doi.org/10.1101/462259; this version posted November 5, 2018. The copyright holder for this preprint (which was not certified by peer review) is the author/funder, who has granted bioRxiv a license to display the preprint in perpetuity. It is made available under aCC-BY-NC-ND 4.0 International license.

Supplementary Fig. 1. *tartan* RNAi in *D. melanogaster* male genitalia. a. Effect on clasper bristle number of UAS-trn TRiP (#28525) or VDRC lines (#5242) combined with the NP6333 driver and controls. Both UAS lines cause a significant reduction in bristle number (UAS-28525 KD p <0.001, $F_{(2,\ 52)}$ = 211.1 and UAS-5242 KD p < 0.001, $F_{(2,\ 39)}$ = 153.9.). Asterisks indicate significant comparisons where p < 0.001. **b**. Effect of *trn* knockdown (using the UAS-trn TRiP line) on *trn* expression in developing claspers compared to controls. Time in hours after puparium formation indicated on the left. Black arrowheads indicate the base of the developing claspers. Boxes show the range, upper and lower quartiles, and the median for each sample.

bioRxiv preprint doi: https://doi.org/10.1101/462259; this version posted November 5, 2018. The copyright holder for this preprint (which was not certified by peer review) is the author/funder, who has granted bioRxiv a license to display the preprint in perpetuity. It is made available under aCC-BY-NC-ND 4.0 International license.

Supplementary Figure 2.

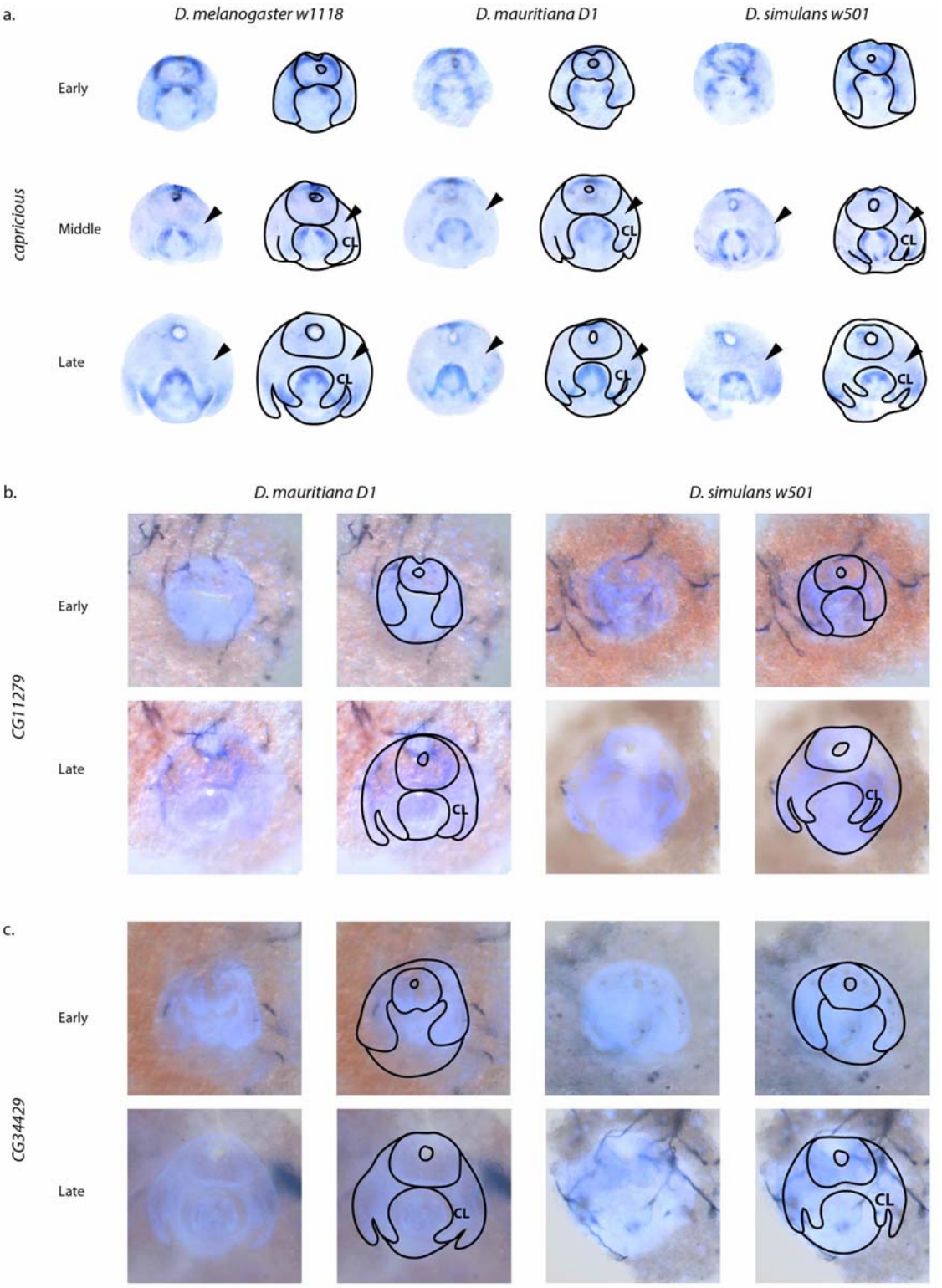

Supplementary Fig. 2. a. Expression of *caps* in the developing male genitalia of *D. melanogaster*, *D. mauritiana* and *D. simulans* during early (approximately 30 to 34 hAPF), middle (approximately 38 to 42 hAPF) and late stages of development (approximately 46 to 50 hAPF). Note that no expression of

bioRxiv preprint doi: https://doi.org/10.1101/462259; this version posted November 5, 2018. The copyright holder for this preprint (which was not certified by peer review) is the author/funder, who has granted bioRxiv a license to display the preprint in perpetuity. It is made available under aCC-BY-NC-ND 4.0 International license.

caps was detectable at the base of the claspers (black arrowheads). Expression of *CG11279* (**b**) and *CG34429* (**c**) in claspers of *D. mauritiana* and *D. simulans* during early (approximately 30 to 34 hAPF), and late stages of development (approximately 46 to 50 hAPF). Note that no expression of these two genes was detected.

bioRxiv preprint doi: https://doi.org/10.1101/462259; this version posted November 5, 2018. The copyright holder for this preprint (which was not certified by peer review) is the author/funder, who has granted bioRxiv a license to display the preprint in perpetuity. It is made available under aCC-BY-NC-ND 4.0 International license.

Supplementary Figure 3.

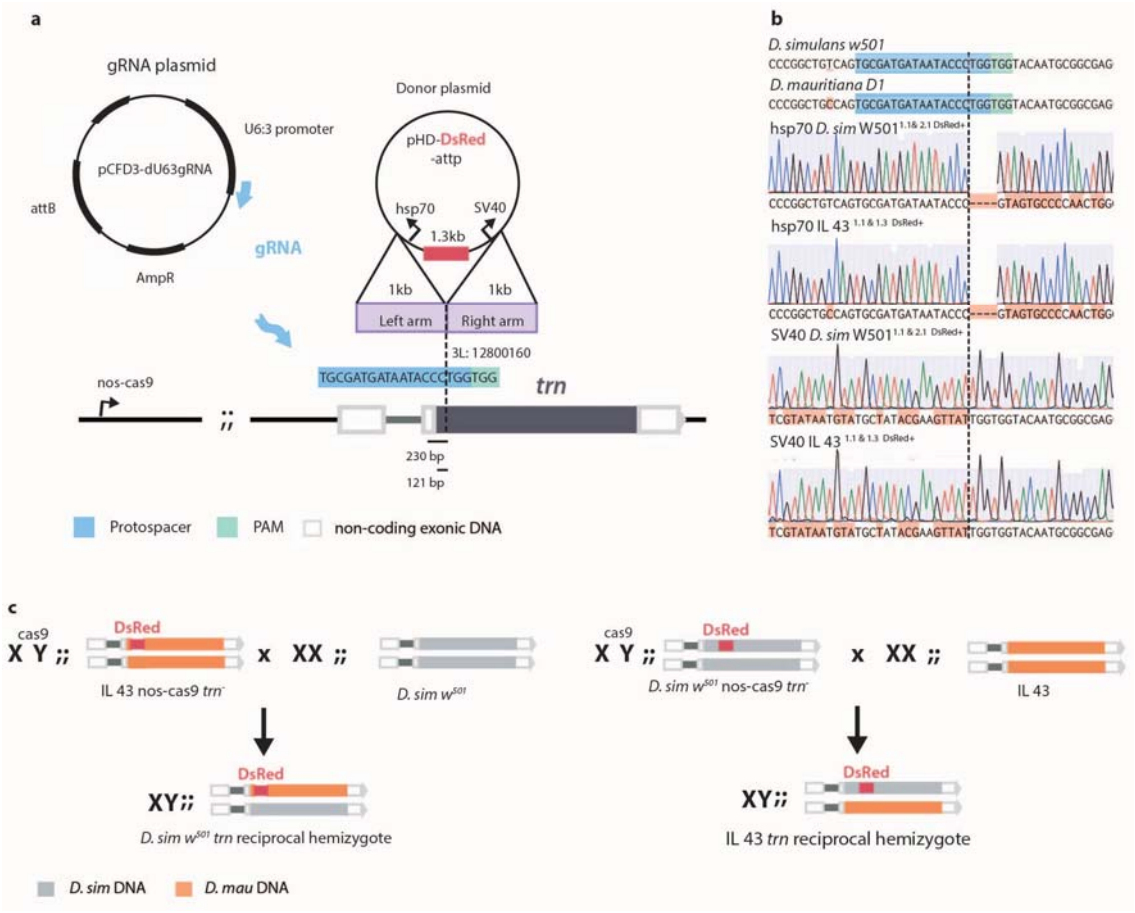

Supplementary Fig. 3. Strategy for generation of *trn* reciprocal hemizygotes of *D. simulans* w^{501} and introgression line (IL) 43 (nanos-Cas9). a. gRNA and donor plasmids used to insert DsRed into the coding region of trn using CRISPR-mediated homologous recombination. **b**. Chromatograms illustrating the disruption of the *trn* reading frames in *simulans* w^{501} and IL 43. **c**. Crossing strategy to generate male reciprocal hemizygotes for *trn*.